TOXICOLOGICAL SCIENCES **132(1)**, 131–141 2013
doi:10.1093/toxsci/kfs337
Advance Access publication January 8, 2013

An *In Vitro* Model of Human Acute Ethanol Exposure That Incorporates CXCR3- and CXCR4-Dependent Recruitment of Immune Cells

Sumera Karim, Evaggelia Liaskou, Samuel Hadley, Janine Youster, Jeff Faint,[1] David H. Adams, and Patricia F. Lalor[2]

Centre for Liver Research and NIHR Biomedical Research Unit, Institute of Biomedical Research, University of Birmingham, Birmingham B15 2TT, UK

[1]Present address: The Binding Site, PO Box 11712, Birmingham B14 4ZB, UK.
[2]To whom correspondence should be addressed. Fax: +44 (0) 121-4158700. E-mail: p.f.lalor@bham.ac.uk.

Received July 4, 2012; accepted December 15, 2012

Alcoholic liver disease (ALD) is one of the commonest causes of cirrhosis and liver failure in the developed world. Hepatic inflammation is the critical stage in progression of both ALD and non-ALD, but it remains difficult to study the underlying mechanisms in a human system, and current animal models do not fully recapitulate human liver disease. We developed a human tissue–based system to study lymphocyte recruitment in response to ethanol challenge. Precision-cut liver slices (PCLS) from human livers were incubated in culture, and hepatic function was determined by albumin production, 3-(4,5-dimethylthiazol)-2,5-diphenyl tetrazolium bromide assay, glucose uptake responses, and morphometric assessment. Responses of tissue and lymphocytes to ethanol exposure were determined by PCR, flow cytometry, histology, and lymphocyte infiltration assays. Human PCLS demonstrated appropriate upregulation of CYP2E1, ADH1α, and ADH3 in response to ethanol treatment. Ethanol also induced expression of endothelial VCAM-1 and ICAM-1, production of sICAM-1 and CXCL8, and the chemokine receptors CXCR3 and CXCR4 on CD4 and CD8 lymphocytes. CXCR3- and CXCR4-dependent migration of lymphocytes into the tissue increased significantly in response to treatment with ethanol. We have demonstrated that ethanol increases chemokine receptor expression and lymphocyte recruitment into human liver tissue, suggesting that it may operate directly to promote hepatitis in ALD. The physiological and pathophysiological responses of the PCLS to ethanol *in vitro* highlight the potential of this assay for dissecting the molecular mechanisms underlying human liver inflammation and as a screening tool for novel therapeutics.

Key Words: **liver; acute toxicity; inflammation; chemokines; hepatocytes.**

Alcoholic liver disease (ALD) is one of the commonest causes of cirrhosis and liver failure in the developed world. The development of hepatic inflammation is the critical stage in disease progression, with infiltration by lymphocytes and neutrophils initiating a cascade of effector mechanisms that ultimately lead to hepatocyte death, fibrosis, and cirrhosis (Haydon *et al.*, 2002). Thus, understanding the molecular mechanisms responsible for early inflammation in alcoholic and nonalcoholic steatohepatitis may identify novel approaches to prevent tissue damage and promote resolution. Animal models of acute ethanol exposure suggest that pharmacological interventions targeting immune cell functions, such as nimodipene (Iimuro *et al.*, 1996) and silymarin (Song *et al.*, 2006) may prevent steatosis and inflammation. Thus, acute models of alcohol exposure have promise for screening novel therapeutic targets and determining modes of action (Massey and Arteel, 2012). Although rodent models of ethanol injury are informative and widely used, they have limitations in that it is difficult to maintain blood alcohol concentrations due to rapid metabolism, and disinclination to voluntarily ingest ethanol requires technically challenging intragastric administration. Thus, we sought to develop a model to study the role of ethanol in acute hepatic inflammation in viable human liver tissue.

Historically, precision-cut liver slices (PCLS) prepared under aseptic conditions have been a valuable tool for the short-term assessment of hepatic biosynthetic and metabolic function. Such models have been used for studies of hepatotoxicity (Beamand *et al.*, 1993; Connors *et al.*, 1990; Price *et al.*, 1996), biotransformation, and metabolism (Heinonen *et al.*, 1996; Muller *et al.*, 2000; Neyrinck *et al.*, 1999; Thohan *et al.*, 2001) predominantly using readily available rodent or small mammal tissue samples. The value of such studies is their ability to measure hepatocyte function in a complex system superior to use of hepatocytes in monoculture. Monocultures are limited by lack of hepatocyte replication in culture and loss of metabolic function and phenotype. Importantly, physiological levels of key proteins such as P450 enzymes fall rapidly during primary hepatocyte culture and may not be accurately represented by tumor-derived cell lines such as HepG2 (Westerink and Schoonen, 2007). PCLS incorporate donor genetic factors and recapitulate the multicellular complexity of the hepatic microenvironment. A small number of studies describe using human PCLS to investigate hepatotoxicity and metabolism

(Connors *et al.*, 1990; Kirby *et al.*, 2004; Price *et al.*, 1996; Wishnies *et al.*, 1991); however (Guyot *et al.*, 2007a,b), few groups have carefully characterized the behavior of human PCLS in culture or used human PCLS to dissect human disease pathogenesis and inflammation. Our aim was therefore to assess the performance of human tissue specimens for generation of viable PCLS and to investigate the potential of this model for investigating human liver inflammation in response to acute ethanol administration. We have shown that nondiseased and diseased human specimens can indeed be used to model early hepatic inflammatory responses to ethanol challenge, and that stimulation of both lymphocytes and the liver microenvironment is necessary to maximally prime recruitment.

MATERIALS AND METHODS

Sample collection and preparation. All patient liver tissue and peripheral blood samples were collected with local NHS research ethics committee approval (Walsall LREC) and written informed consent. Donor liver tissue surplus to transplantation requirements, "normal" tissue margins from livers removed during tumor resection surgery, and explanted liver tissue from patients being transplanted for end-stage chronic liver disease (e.g., primary biliary cirrhosis [PBC] and ALD) were collected from the Queen Elizabeth Hospital, Birmingham, United Kingdom. For generation of PCLS, cores were cut from the tissue immediately upon receipt of tissue in the laboratory. On occasion, cores were briefly stored in Dulbecco's Modified Eagle Medium (DMEM, Invitrogen, United Kingdom) at 4°C prior to slicing. A Krumdieck Tissue Slicer (Alabama Research and Development) was set up according to manufacturer's instructions and filled with sterile PBS. The core was placed into the slicer assembly under aseptic conditions, and circular slices of ~240 µm thickness were generated with a blade cycle speed of 20–70 min^{-1} (see later) and collected into the sterile media reservoir. Upon generation of sufficient slices for experimentation, samples were immediately transferred into culture media composed of Williams E media (Sigma, United Kingdom) supplemented with 2% fetal calf serum (FCS, Invitrogen), 0.5µM insulin, and 0.1µM dexamethasone (Guyot *et al.*, 2007a,b). These supplements were omitted from culture media for glucose uptake assays. PCLS were cultured for up to 48 h either in a 24-well plate or in a tissue culture insert suspended in a 24-well plate (BD Biosciences, 0.8 µm pore size) at 37°C, in a 5% CO_2 incubator. Where indicated, PCLS were cultured in media containing ethanol (50–200mM, media was replaced every 8 h to minimize effects of ethanol evaporation), tumor necrosis factor-α (TNF-α, 100 ng/ml), or lipopolysaccharide (LPS, Sigma, 1 µg/ml) for 24 h. Prior to snap freezing and cryosectioning of treated PCLS into 15µM histological sections, they were fixed in formyl saline and incubated in 30% sucrose according to standard protocols. Peripheral blood lymphocytes (PBL) were isolated from normal donors using Lympholyte density gradient (Cedarlane, VH BIO Ltd, United Kingdom) according to manufacturer's instructions, and contaminating monocytes were depleted by virtue of their adhesion to plastic. Cells were resuspended in RPMI medium containing 1% FCS (Invitrogen) prior to use. The JY lymphocytic cell line was a kind gift from Dr Nick Pullen at Pfizer, United Kingdom and was cultured in RPMI medium containing 10% FCS as previously described (Liaskou *et al.*, 2011). These cells are commercially available via the ATCC.

Assessment of PCLS functional integrity. Viability of PCLS in culture was determined using 2 mg/ml 3-(4,5-dimethylthiazol)-2,5-diphenyl tetrazolium bromide (MTT, Sigma). Slices were incubated with MTT at 37°C for 1.5 h and washed, and dye was solubilized using dimethylsulfoxide (DMSO). Absorbance of replicate samples and DMSO background control were read at 570 nm. Mean absorbance was expressed per 500 mg of tissue. Hepatocyte function was assessed by measuring albumin production by ELISA using optimal concentrations of coating antibody (antihuman albumin antibody) and detection antibody (horseradish peroxidase–conjugated antihuman albumin antibody: both Bethyl Industries) and albumin standards (Bethyl Industries). Standards and triplicate supernatants were incubated in wells for 1 h and all washes were performed with Tween containing 0.2% FCS. Binding of detection antibody was visualized with TMB substrate (Sigma), and the reaction was stopped using 2.5M H_2SO_4 prior to reading at 450 nm. Albumin concentration in samples was determined by comparison to standard concentration curve. To quantify glucose uptake, freshly cut slices were removed from complete media and cultured in 500 µl low-glucose DMEM (Invitrogen), 2% FCS for 2 h. After washing, media was replaced with DMEM containing stimulants 0.10 IU insulin or media alone for 2.5 h, followed by incubation for 30 min with 500 µl DMEM containing 0.1mM 2-deoxyglucose and 2 µci/ml 2-deoxy-D-glucose [3H (G)] (both Sigma). PCLS were washed three times with ice-cold PBS, and tissue was lysed in 400 µl of 1N NaOH (Sigma). Microscopic assessment was performed to ensure adequate cell lysis, and tissue was mixed with 4 ml of scintillation fluid (Fisher Scientific, United Kingdom) prior to scintillation counting. Data were normalized to represent 2-deoxy-D-glucose [3H (G)] uptake (DPM) per 500 mg of tissue.

Histological staining of sections. Cryosections of 15µM cut from PCLS were counterstained with hematoxylin and eosin (Leica, United Kingdom) according to standard protocols. For assessment of glycogen content, sections were stained using periodic acid-Schiff stain (Leica) using standard methodology. Nuclear integrity was assessed using bisbenzimide (Hoescht dye, 2.5 µg/ml, Sigma) staining followed by fluorescent microscopic imaging. Cryosections prepared from PCLS were also stained using standard immunohistochemical staining techniques with DAB substrate. After blockade of endogenous peroxidase activity (0.3% hydrogen peroxide in methanol, Sigma), predetermined optimal concentrations of primary antibody directed against CYP2E1 (AbCAM, 1/2000), ADH (Biogenesis, 1:2000), ADH1α, ADH3 (both Proteintech, 6 µg/ml), VCAM-1, and ICAM-1 (both R+D systems, United Kingdom, 10 µg/ml) were incubated on sections for 1 h. Primary antibody binding was detected using a species-specific secondary antibody-peroxidase reagent kit (ImmPRESS, Vector Labs, United Kingdom) according to manufacturer's instructions. Finally, sections were visualized with a peroxidase substrate kit (ImmPACT DAB, Vector Labs) and counterstained with hematoxylin. Isotype- and species-matched antibodies were used as controls, and representative images were captured using Zeiss Axiovision software (Zeiss, United Kingdom).

PCR. Freshly cut PCLS or PCLS that had been cultured under various conditions were stored in RNALater (Sigma) at 4°C until RNA extraction using an RNeasy mini kit (Qiagen) according to manufacturer's instructions. RNA concentration and purity were assessed and samples were stored at −80°C. cDNA was generated from each sample using a cDNA synthesis kit (BioRad, United Kingdom) according to manufacturer's instructions. All samples of cDNA were diluted to 200 µg/ml. Twenty microliters of PCR master mix were prepared on ice for each sample (1× Green GoTaq Flexi buffer, 1mM $MgCl_2$, 0.2mM dNTPs, 0.25 pmol/µl primer, 1.25 U GoTaq DNA polymerase [all from Promega, Southampton, United Kindgom], and 10 µg/ml cDNA in ddH_2O) and run for 35 cycles as follows: 95°C for 2 min, denaturation at 94°C for 30 s, a variable annealing temperature specific for each primer for 1 min, and a final extension step of 72°C for 45 s followed by 72°C for 5 min. Ethidium bromide–labeled products were visualized by electrophoresis in an agarose gel (95–130 V for 30–45 min), and images were captured under UV illumination using GeneSnap software. Densitometric analysis of product intensities relative to GAPDH signal in similarly treated samples was performed using Image J. Primer sequences used are given in Table 1.

Flow cytometry. Lymphocytes collected from cultured PCLS supernatants were incubated with fluorescently conjugated mouse monoclonal antibody (CD3-PE, CD4-FITC, CD8-FITC, CD14-APC, CD16-FITC, and CD19-PE; CCR5-PE, CXCR3-PE, and CXCR4-PE; or species- and isotype-matched control, Serotec, United Kingdom) at optimal concentrations (typically 1–10 µg/ml) for 30 min on ice. Where indicated, lymphocytes were preincubated with 50–100mM ethanol prior to labeling. Cells were washed in PBS, resuspended in 10% FCS/PBS, and analyzed on a Beckman Coulter Epics XL cytometer

TABLE 1
Primers Used for Semiquantitative PCR Analysis

Product	Annealing temperature (°C)	Sequence
ADH1	51.5	F 5′-AGTCATCCCACTCGCTATTCC-3′ R 5′-GTCCCCTGAGGATTGCTTACA-3′
ADH3	51.5	F 5′-GCTTTAAGAGTAAATAATCTGTCCCC-3′ R 5′-ATTCTACCTCTTTCCAGAGC-3′
ICAM-1	58	F 5′-TCTGTGTCCCCCTCAAAAGTC-3′ R 5′-GGGGTCTCTATGCCCAACAA-3′
E-Selectin	53	F 5′-GATGAGAGGTGCAGCAAGAAG-3′ R 5′-CTCACACTTGAGTCCACTGAAG-3′
GAPDH	55	F 5′-AAT GTC ACC GTT GTC CAG TTG-3′ R 5′-GTG GCT GGG GCT CTA CTT C-3′

running System II software (Beckman Coulter). Median channel fluorescence (MCF) values and percentage positivity were determined for each marker relative to isotype control staining.

Cytokine secretion assays. The secretion of a variety of cytokines from PCLS treated with 100mM ethanol for 24 h was tested using the Proteome Profiler Human Cytokine Array Kit (Panel A, Invitrogen), according to manufacturer's instructions. Supernatants were collected from control and ethanol-treated slices after 24 h in culture and diluted 10-fold prior to immobilization on the assay membrane. The assay was developed according to manufacturer's instructions, and densitometric analysis of protein spots was performed using Image J. Data expressed as relative spot intensity from four replicate samples of two liver donors.

Lymphocyte adhesion and infiltration assays. The adhesion of lymphocytes to frozen tissue sections (10 µm) cut from control and treated PCLS was determined using a modified Stamper-Woodruff adhesion assay as previously described (Lalor *et al.*, 2010). Lymphocyte (1×10^6 cells/ml) binding to endothelium (sinusoidal and vascular compartments) was examined microscopically and expressed as mean adherent lymphocytes per high-powered field by counting 15 fields randomly. Additional experiments were performed using a higher starting cell count (5×10^6 cells/ml) to assess effects of chemokine receptor inhibition on adhesion. Here, PBL were pretreated with 10 µg/ml of mouse antihuman CXCR3- or CXCR4-blocking antibodies (R+D systems) for 30 min prior to performing assay. For assessing infiltration of lymphocytes into cultured ethanol-treated PCLS, lymphocytes were labeled with Cell Tracker Green (Molecular Probes) according to standard protocols (Johnson *et al.*, 2006), resuspended to 2×10^6 cells/ml, and incubated directly onto slices in the presence or absence of 50–100mM ethanol for 24 h in complete media. After fixation in formyl saline, serial sections were immediately snap frozen and cut into sequential 10µM cryosections, were labeled with bisbenzimide, and were imaged as above. Numbers of CTG-labeled cells present per high-power field (HPF) of sequential sections were calculated as before.

Statistical analysis. Data were analyzed using paired or independent Student's *t*-test or one-way ANOVA followed by Bonferroni's multiple comparison posttest. A value of $p < 0.05$ was considered statistically significant.

RESULTS

Human PCLS Remain Functional and Morphologically Intact in Static Culture

Little experience using the Krumdieck tissue slicer with human liver specimens has been reported. We have used human liver tissue to generate tissue cores that were then cut into PCLS from 36 human liver specimens (9 normal donor tissue, 19 resection margin specimens, and 8 end-stage liver explants). We were able to cut sections from most liver diseases although severely cirrhotic liver tissue and samples from patients with end-stage PBC were least amenable to cutting. Extremely fatty donor specimens were difficult to cut and resisted extraction through the machine; however, we overcame this problem by prechilling the tissue core at 4°C for 30 min prior to cutting into chilled media. Slice weights in any experiment were consistent (mean slice weight = 31.87 mg ± 8.65%, 57 slices from five different livers). Slices were cultured in Williams E media supplemented with insulin, dexamethasone, and FCS either in 24-well plates or on 24-well culture inserts suspended in well plates at 37°C in a 5% CO_2 incubator. Functional activity was maintained at 24 h as evidenced by production of albumin and MTT reduction (Figs. 1A and B), and we noted no difference in viability for slices cultured in wells versus culture inserts (MTT signals = 10.26 ± 0.22 vs. 12.53 ± 0.7/500 mg of tissue, respectively). Interestingly, we noted that although viability of normal and cirrhotic specimens was similar up to 24 h in culture (Fig. 1B), there was a rapid decline in function of cirrhotic specimens thereafter. Thus, for all subsequent functional experiments, we restricted our use of tissue specimens to those from normal tissue or resection margin specimens. We noted that resident red blood cells and leukocytes from the tissue, and also lipid in particularly fatty specimens migrated from the cut faces of the tissue into the culture media surrounding PCLS overnight as we have previously reported (Goddard *et al.*, 2004). The exuded leukocytes which numbered 100,000 per slice included CD3+, CD4+, CD8+, and CD19+ lymphocyte populations as well as small numbers of CD14+ monocytes (Supplementary fig. 1). Nuclear integrity of hepatocytes as shown by bisbenzimide staining and morphometric analysis was maintained at 24 h, with a tendency to decrease in central areas of the slice during longer culture (Figs. 1C and D). Morphology was maintained during culture of up to 48 h and was excellent at 24 h in static culture (Fig. 1E). Radiolabeled glucose uptake assays confirmed that PCLS retained ability to respond to insulin at 24 h (Fig. 1F), and staining of sections cut from cultured slices confirmed the presence of glycogen granules at 24 h, which decreased with prolonged culture (Fig. 1F).

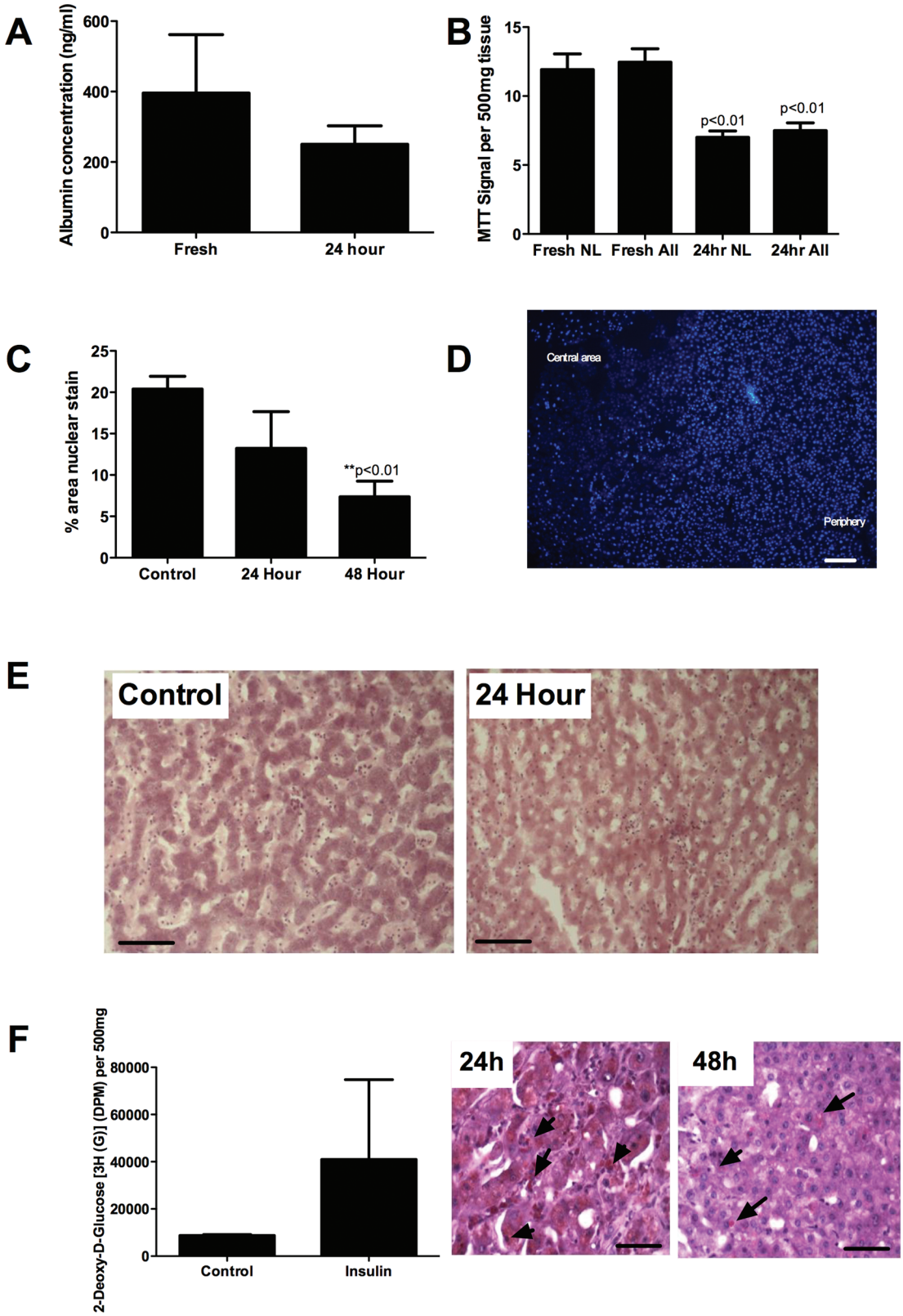

FIG. 1. (A) Production of albumin by cultured liver slices (six representative slices from three different liver specimens) measured by capture ELISA. Paired *t*-test showed no significant difference between control and 24 h incubations ($p = 0.4$). (B) MTT reduction assay using between 40 and 56 replicate slices from normal and resection margin tissue only (NL) or all liver (ALL) slices, which included slices from five end-stage cirrhotic specimens. Paired *t*-test showed no significant difference between signal from normal livers and all livers and a significant reduction in signal at 24 h compared with control. Data represent signal normalized per 500 mg of tissue ± SEM for triplicate slices from each liver. (C) Image J quantification of images from representative fields of view captured from

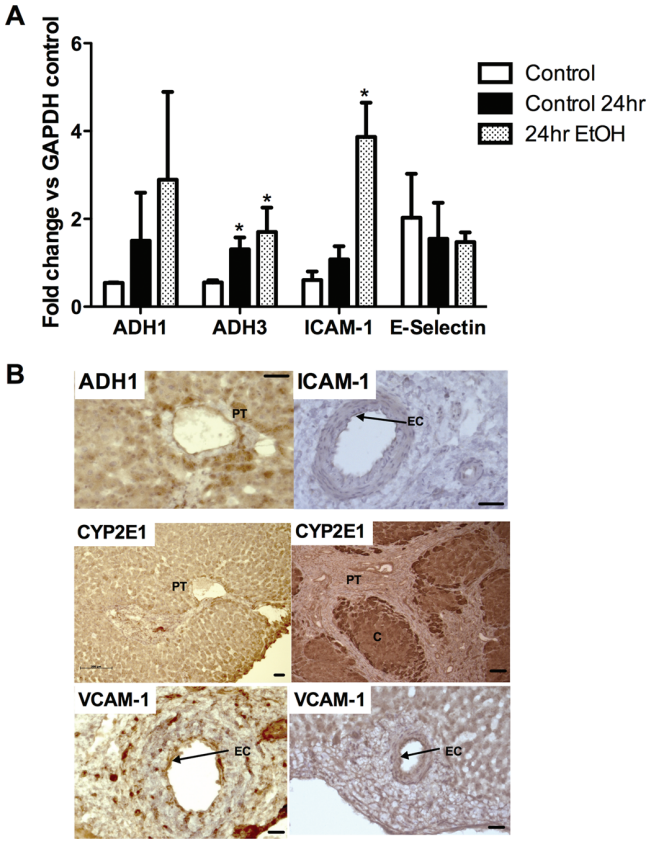

FIG. 2. (A) Semiquantitative PCR data from representative PCLS from three liver specimens: fresh liver (control), samples cultured in media alone (control 24 hr), and 100mM ethanol (24 hr EtOH) for 24 h prior to RNA extraction. Data represent mean ± SEM densitometric signal for ADH1, ADH3, ICAM-1, and E-Selectin expressed as a fold change relative to expression of housekeeping gene. *Paired *t*-test indicates significant increase in expression relative to control $p < 0.05$. (B) Representative histological staining from samples of the same treated PCLS (i–iii) or of liver from a patient with ALD (iv) showing localization of positive signal for ADH1 (PT = portal tract, brown staining localized to periportal hepatocytes), ICAM-1 (EC = endothelial cells in portal vessel staining positive), and CYP2E1 (localized brown staining throughout lobule in PCLS and localized to periportal areas in ALD liver, PT = portal tract and C = central area of lobule) and expression of VCAM-1 (EC = endothelial cells in portal vessel) on untreated (v) and treated (100mM, 24 h) (vi) PCLS. Samples were stained using standard immunohistochemical methods and DAB chromogen, and isotype controls were negative (not shown). Bars indicate 50μM.

Human PCLS Respond to Ethanol Treatment in Culture

Next we used PCLS as microscale models to study the effects of ethanol on inflammatory cell recruitment into human liver tissue. All functional readouts measured after ethanol treatment were compared with baseline values for slices that had been cultured under the same conditions in the absence of ethanol. Treatment of slices with relevant concentrations of ethanol for 24 h had no effect on viability (not shown) and resulted in upregulation of ADH1α and ICAM-1 at mRNA and protein level (Figs. 2A and B). We also noted induction of ADH3 (Fig. 2A). ADH1α and ADH3 were expressed predominantly in hepatocytes, particularly in periportal cells, although we noted some endothelial expression upon ethanol stimulation (representative image of ADH1 staining in Fig. 2B), and similarly endothelial expression of ICAM-1 was markedly increased upon stimulation. We also observed an induction of CYP2E1 in hepatocytes in response to ethanol treatment as expected, but interestingly expression was uniform across the lobule and did not demonstrate the zonal variation seen in ALD tissue (Fig. 2B). VCAM-1 and E-Selectin expression was also studied, and although we noted increased staining of slices upon treatment (Fig. 2B, bottom panels), there was considerable donor- and disease-dependent variation in basal expression and thus PCR showed no significant effect of ethanol on expression (e.g., E-Selectin, Fig. 2A).

Ethanol Treatment Increases Production of Soluble Adhesion Molecules and Chemokines by Human Liver Slices and Modulates Chemokine Receptor Expression on PBL

In parallel with our observed increases in adhesion molecule expression in ethanol-treated slices, we measured secretion of proinflammatory molecules into the culture supernatants. We detected secretion of the immunomodulatory chemokines MIF, CXCL8 (IL-8), and CXCL1 (GROα) from PCLS, and in particular increased levels of sICAM-1 and IL-8 (CXCL8) secreted into the media of alcohol-treated tissue slices (Fig. 3). There was also a tendency for reduced production of IL-16. We did not detect any significant secretion of the CXCR3 ligands CXCL9-11. Cytometric analysis of CD4+ and CD8+ lymphocytes exposed to ethanol at concentrations matching those used during the coincubation with PCLS demonstrated that stimulation resulted in significant upregulation of the chemokine receptors CXCR3 and CXCR4 (Fig. 4) by the lymphocytes. We also noted occasional upregulation of CCR5 in some patients, but here magnitude of effects varied with donor and duration of ethanol exposure. We studied the effect of ethanol treatment on lymphocyte adhesion to and migration into PCLS.

Ethanol Treatment Increases Recruitment of Lymphocytes to Liver Tissue

In static, tissue-binding assays, we noted a concentration-dependent increase in PBL (Fig. 5A) adhesion to endothelium

←

normal sections stained using bisbenzimide to visualize nuclear integrity. Data represent mean ± SEM% of area stained positive in five HPF analyzed for duplicate slices from four liver samples. Paired *t*-test revealed significant reduction in nuclear number at 48 h. (D) Representative image from stained normal liver after 48 h in culture showing loss in nuclear integrity in central area of slice compared with periphery. Bar represents 100 μm. (E) Representative images showing gross morphology of parenchymal areas of sections cut from PCLS collected fresh (Control) or cultured in a well for 24 h (24 Hour) stained using hematoxylin and eosin (original magnification ×200, bar represents 50 μm). (F) Uptake of radiolabeled glucose in response to insulin treatment of normal PCLS. Data represent mean ± SEM uptake of six replicate slices (left graph) and periodic acid-Schiff stain of sections from representative PCLS confirming the presence of glycogen granules after 24 and 48 h in culture (right figures). Glycogen stains a reddish purple (see samples indicated by arrowheads), and bar represents 50 μm.

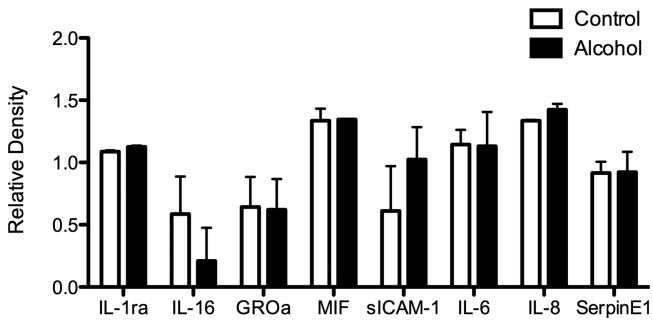

FIG. 3. (A) Production of proadhesive mediators by human PCLS in response to ethanol exposure. PCLS from two representative donors (one normal and one diseased) were incubated for 24 h in the absence (white bars) or presence (black bars) of 100mM ethanol, and secretion of mediators into supernatants was measured using a cytokine profiler kit according to manufacturer's instructions. Data represent mean + SD relative intensity of spots from four samples.

in tissue slices that had been treated for 24 h with ethanol. This effect was similar in magnitude to that observed if slices were treated with TNF-α (not shown). However, enhanced adhesion was only seen with concentrations of ethanol above 100μM, and the increase in adhesion was small. In contrast, when we incubated both lymphocytes and PCLS with ethanol during an infiltration assay (Fig. 6A), marked increases in lymphocyte infiltration were noted even in response to 50mM ethanol. Of note, when we combined our ethanol treatment with exposure to LPS to mimic transit of bacterial products to the liver *in vivo* following ethanol challenge (Supplementary fig. 2), we observed no increase in immune cell binding above that seen following ethanol treatment alone. We observed the majority of adhesion events localized to the periphery of PCLS, but during the 24-h incubation period migrating cells were able to penetrate some distance into the parenchyma (Fig. 6B, arrows). When we performed adhesion assays using ethanol-treated slices in the presence of chemokine receptor–blocking antibodies, we observed a significant inhibition of adhesion when both CXCR3 and CXCR4 were blocked (Fig. 6C, 38% decrease in adhesion) and also a trend for reduction in binding in the presence of the single antibodies (Fig. 6C).

DISCUSSION

We have demonstrated that cultured PCLS generated from explanted human liver specimens retain morphological and functional capacities for up to 48 h in static culture. This represents one of the first examples of prolonged functional studies using normal human liver slices in culture although other groups have reported elegant examples of slices from liver and other organs supporting replication of therapeutic viral vectors (Kirby *et al.*, 2004; van Geer *et al.*, 2009). Our data support the use of human PCLS in preclinical efficacy studies, with the advantages of recreating the hepatic mileu and incorporation of interdonor and disease-specific variability. We compared the performance of normal tissue samples with that of explanted livers from patients with end-stage cirrhotic liver disease, and although viability of slices was similar up to 24 h, decline thereafter was more rapid in diseased specimens, which precluded their use for the majority of our functional experiments. This is consistent with our laboratory's experience of isolating primary human hepatocytes, which is more difficult from end-stage samples from patients with advanced cirrhosis (Bhogal *et al.*, 2011). Bile salts from cholestatic specimens may promote hepatocyte apoptosis (Faubion *et al.*, 1999), and similarly leaching of free fatty acid into the slice supernatant may induce lipoapoptosis (Cazanave and Gores, 2010). We were able to collect significant numbers of leukocytes from diseased sample supernatants as previously reported (Goddard *et al.*, 2004), and local cytokine release from such resident immune cells or activation of leukocytes in inflamed samples may also promote apoptosis in diseased liver samples. Furthermore, our experience with using diseased tissue for measurement of adhesion of leukocyte and stem cells in Stamper Woodruff adhesion assays (Aldridge *et al.*, 2012; Edwards *et al.*, 2006) confirms that variations in endogenous adhesion molecules and chemokine expression alter basal binding in the absence of exogenous stimuli making the assessment of additional effect of ethanol stimulation more challenging.

Our culture system is based upon incubation of slices in wells or on tissue culture insert supports for up to 48 h. Morphological evidence and functional albumin secretion, MTT reduction, and glucose uptake, as well as responses to ethanol and cytokine treatment, confirm that viability is maintained for this period. This extends the duration of much reported evidence using rodent slices for toxicological and metabolic studies, where culture durations of a few hours are not uncommon (Mortensen and Dale, 1995; Naik *et al.*, 2004) and where visual assessment of tissue integrity is not always performed. However, we acknowledge that between 24 and 48 h, we began to observe central necrosis of slices both in wells and on supports with decreased nuclear integrity and loss of morphological structure compared with the periphery of the section that maintained adequate media perfusion and gaseous exchange. This was associated with a fall in albumin secretion. Other groups have also demonstrated a gradual loss in expression of CYP450 enzymes associated with culture of human liver slices (Martin *et al.*, 2003). Such effects have been minimized in rodent studies by immobilizing slices on tissue supports in roller bottles (Clouzeau-Girard *et al.*, 2006; Guyot *et al.*, 2007a,b) or in microchamber perfusion devices (van Midwoud *et al.*, 2010). We are currently adapting our system to incorporate a similar perfusion device, but in the current investigation all of our functional assays were done within 24 h to ensure maximal viability.

After exposure of human PCLS to 100mM ethanol for 24 h, we did not observe significant changes in structural or nuclear morphology as has been reported in rodent PCLS after acute exposure to higher concentrations of ethanol (Naik *et al.*, 2004). Ethanol of 100mM is at the high end of what is

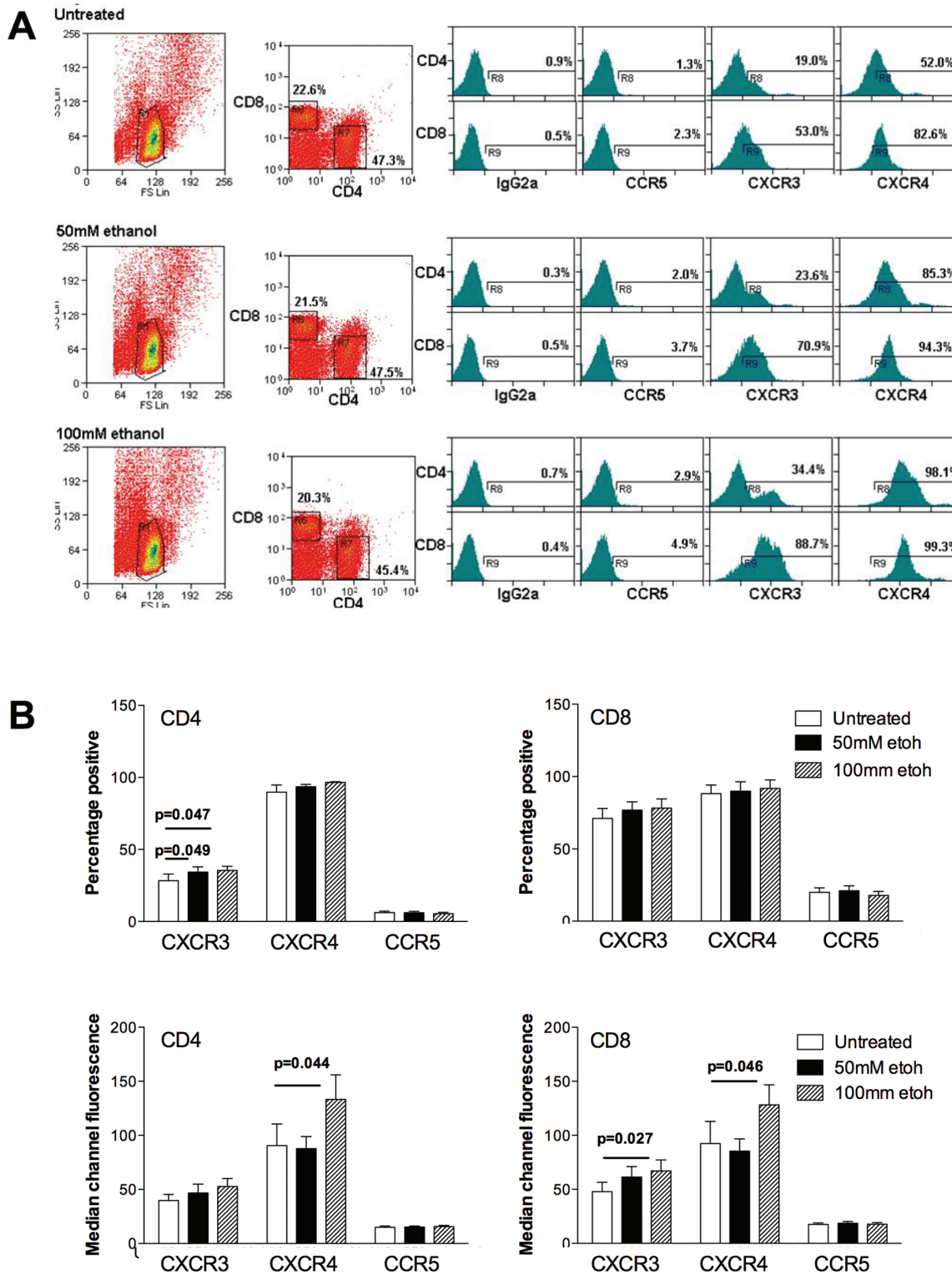

FIG. 4. Exposure of lymphocytes to ethanol modulates chemokine receptor expression. (A) Typical flow cytometric analysis of a representative sample of normal PBL which were maintained in culture in media alone (untreated) or indicated concentrations of ethanol (50–100mM) in complete media. Cells were gated on FS/SC (left panels); expression of CD4 and CD8 (central panels); and expression of the chemokine receptors CCR5, CXCR3, and CXCR4 (histograms). Data represent percentage of CD4 and CD8 cells positive for indicated chemokine receptor and expression was determined relative to indicated isotype controls. (B) Pooled data for expression of the chemokine receptors CCR5, CXCR3, and CXCR4 indicated by percentage positive cells and MCF values for CD4 (left graphs) and CD8+ (right graphs) lymphocytes from seven donors. Data represent mean ± SEM, and bars indicate significant differences between control and ethanol-treated lymphocytes.

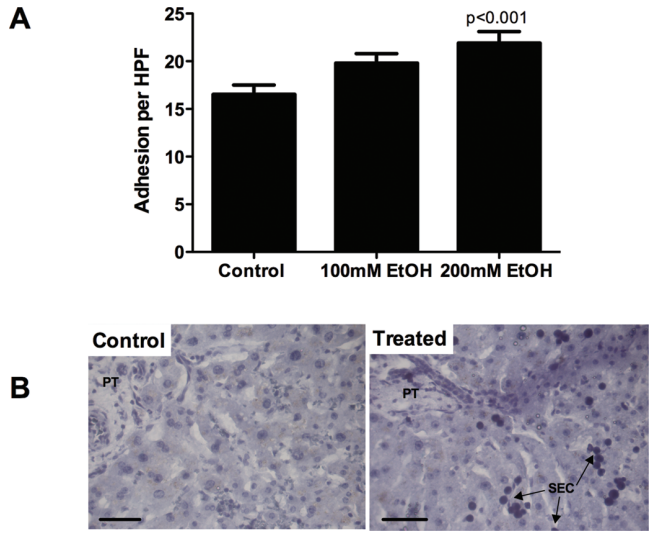

FIG. 5. Adhesion of PBL (A) to cryosections cut from PCLS treated with media alone, ethanol (100–200mM), or TNF-α (20 ng/ml) for 24 and 4 h, respectively. Data represent mean ± SEM adhesion to endothelial structures per HPF. Representative images from a typical control and treated sample are shown (B). Bar represents 50μM, and PBL localize to endothelial cells in sinusoids (SEC).

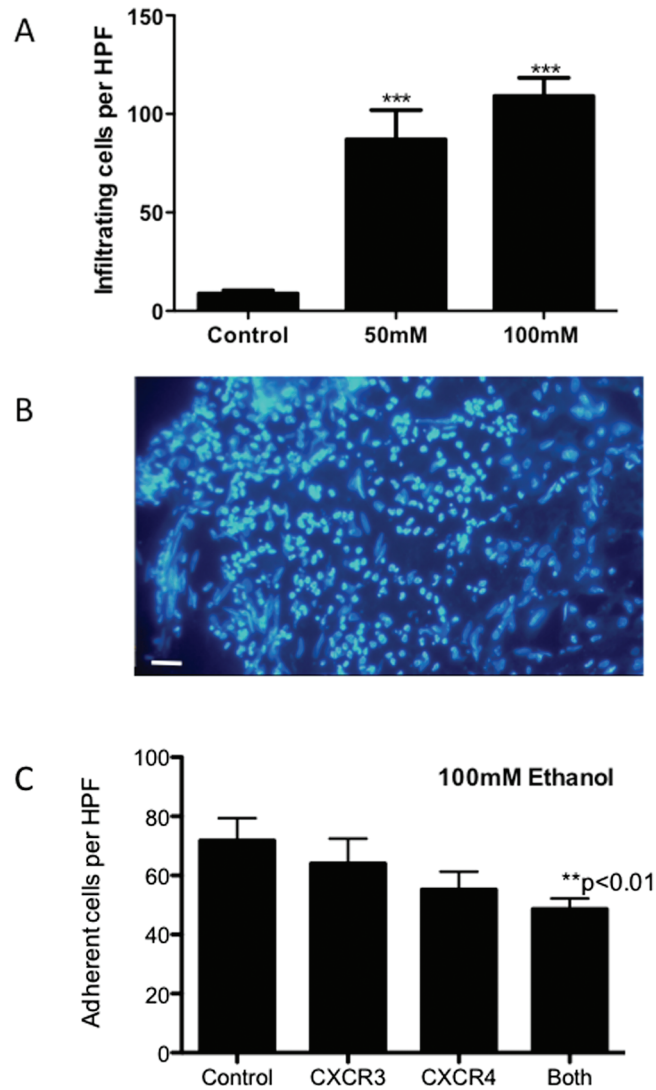

FIG. 6. (A) Infiltration of CellTracker Green–labeled lymphocytes into PCLS in the presence of ethanol. Labeled lymphocytes were incubated with PCLS in the absence (control) or presence of indicated concentration of ethanol (50–100mM) for 24 h in complete media. Data represent mean ± SEM number of infiltrating cells per HPF of view (n = 15 samples from duplicate slices) Paired t-test confirms that alcohol pretreatment significantly increases lymphocyte infiltration (***$p < 0.001$). (B) Representative image of the edge of a treated PCLS showing predominant localization of labeled cells to the periphery with occasional cells infiltrating central areas (white arrows). Bar represents 50μm. (C) Adhesion of PBL to cryosections cut from PCLS treated with ethanol (100mM) for 24 h. Lymphocytes were untreated or treated with 10 μg/ml of CXCR3 or CXCR4 mab, or a combination of the two ("both") as indicated. Data represent mean ± SEM adhesion to endothelial structures per HPF in three replicate experiments using three liver donors, and paired t-test indicated significant reduction in adhesion when lymphocytes were treated with both antibodies compared with control (**$p < 0.01$)

measured in intoxicated humans although standard in many *in vitro* culture systems (Donohue *et al.*, 2006; Xu *et al.*, 2003) and equivalent to blood and urine alcohol levels achieved by intragastric administration in rats (Ronis *et al.*, 2004). Of note, even with regular replacement of media in our cultures, it is likely that the effective concentration within PCLS is likely to be lower than 100mM as we have observed up to 30% decrease in effective concentration over 24 h due to evaporation in cell free wells (not shown). This is of interest because we may be incidentally mimicking physiological discontinuous exposure patterns caused by patterns of sleep or weekend consumption of alcohol, which are associated with reduced systemic oxidative stress but enhanced immune activation in animal models compared with continuous exposure (Fernandez-Mateos *et al.*, 2012). However, we would need to compare maintained exposure and interrupted exposure using a perfusion delivery system to assess whether such patterns of exposure alter immune cell recruitment in the human system. Nevertheless, ethanol treatment resulted in upregulation of CYP2E1 (Cohen *et al.*, 1997; Cohen and Nagy, 2011; Wu and Cederbaum, 2005) across the liver lobule. *In vivo*, ethanol administration leads to a zonal distribution (Cohen *et al.*, 1997) of CYP2E1, and the uniform induction in our system is likely to be a consequence of the uniform diffusion of ethanol across the whole slice rather than directed delivery through the blood supply. Similarly, we observed a global upregulation of ADH1α, the enzyme typically responsible for acute metabolism of moderate doses of ethanol (Haseba and Ohno, 2010), the high K_m variant ADH3 that is more important during chronic or high-dose exposure (Haseba and Ohno, 2010), and a more localized endothelial induction of VCAM-1 and ICAM-1 expression. This supports data from patients with alcoholic hepatitis in whom increased expression of ICAM-1 is observed on venous and sinusoidal endothelium as a consequence of local proinflammatory cytokines particularly TNF-α (Burra *et al.*, 1992; Lalor *et al.*,

2007) and is important for immune cell recruitment (Kono *et al.*, 2001). It is likely that resident Kupffer cells and monocytes/macrophages represent the local source of TNF-α following ethanol exposure (Cohen and Nagy, 2011). The data also correlate well with increased secretion of sICAM-1 into tissue culture supernatants following ethanol exposure and increases noted in patients who consume alcohol (Sacanella *et al.*, 1999). We also see a reduction in secreted IL-16 in accordance with a reported reduction in serum levels observed in humans given alcohol (Chiva-Blanch *et al.*, 2012).

The increased expression of adhesion molecules in response to ethanol has functional implications, because the adhesion of lymphocytes to endothelial cells within fixed sections from PCLS was enhanced following ethanol exposure to a level comparable to that seen with exogenous administration of TNF-α. In patients, it is likely that alterations in gut permeability in response to ingestion of alcohol lead to concurrent delivery of bacterial products such as endotoxin to the liver via the portal circulation (Saito and Ishii, 2004) that may have additional immunomodulatory effects. Single exposure of sinusoidal endothelium to endotoxin results in downregulation of T-cell costimulatory function via decreased Class II, CD80 and CD86 expression (Knolle *et al.*, 1999). Furthermore, ethanol treatment of whole blood has been demonstrated to blunt subsequent leukocyte integrin upregulation in response to LPS treatment (Ozaki *et al.*, 2007) and can reduce endocytosis and cytokine production by immune cells (Andrade *et al.*, 2009). However, repeated stimulations of sinusoidal endothelium (as would be experienced by persistent drinkers) lead to blunting of responses, downregulation of adhesive receptor expression, and tolerance of liver sinusoidal endothelial cells to stimuli as a means of controlling local inflammation. These responses are difficult to model, but when we assessed the effects of a single 24 h costimulation of PCLS with ethanol and LPS on immune cell recruitment, we noted no additional effects of LPS on recruitment. This suggests that in the short term, LPS does not modulate the ability of hepatic endothelium in tissue slices to recruit immune cells, but it would be interesting to investigate whether subsequent functions of recruited cells are impaired. A more pronounced response occurred when both tissue and inflammatory cells were exposed to ethanol in coculture. Here, local expression of adhesion molecules and chemokines within tissue was accompanied by enhanced expression of CXCR3 and CXCR4, and occasionally CCR5 on ethanol-exposed lymphocytes. Cyclic AMP–dependent modulation (Boyadjieva and Sarkar, 1999) of chemokine receptors on lymphocytes in response to alcohol has been described previously and linked to susceptibility to HIV infection in alcoholics (Liu *et al.*, 2003; Wang *et al.*, 2002). More importantly, these receptors recognize ligands that are upregulated during human liver inflammation (Oo *et al.*, 2010; Tacke *et al.*, 2011), and in particular ligands for CCR5 are upregulated in response to ethanol in humans (Yeligar *et al.*, 2009; Zhang *et al.*, 2003) and in murine models (Jaruga *et al.*, 2004). We screened for enhanced secretion of ligands for these chemokine receptors in supernatants from tissue slices but interestingly noted that apart from CXCL8, we did not detect any significant secretion of CXCR3 ligands. This may reflect the fact that locally produced chemokine becomes immobilized on the endothelial glycocalyx (Curbishley *et al.*, 2005) to support localized lymphocyte recruitment. Thus, it is likely that a combination of enhanced local production of proadhesive/migratory ligands within tissue and chemokine receptor expression on inflammatory cells supports enhanced CXCR3- and CXCR4-dependent recruitment of lymphocytes into our ethanol-exposed PCLS.

We have confirmed that human liver tissue slices from normal and fibrotic/cirrhotic specimens can be sliced and maintained in culture for up to 48 h and respond appropriately to alcohol treatment *in vitro*. Although this time course has the advantage of permitting analysis of the as-yet poorly defined early cellular responses to ethanol treatment, particularly the activation of profibrotic cells (Guyot *et al.*, 2007a,b, 2010), it is likely that modifications to the culture protocol described to include either perfusion of media or incubation of slices on supports within rotary culture (Klassen *et al.*, 2008; Schaffert *et al.*, 2010) will further extend the period of maximal viability in culture. We can also begin to dissect the interplay between parenchymal cells, the immune system, and other hepatic cells using this model, and our access to both "normal" and fibrotic liver specimens permits comparisons to be drawn between pathogenic mechanisms in "naïve" and alcohol-sensitized liver. We can also operate using tissue with appropriate patterns of fibrosis, which are hard to achieve in many drug-induced rodent models and which do not occur in response to intragastric administration of ethanol (Schaffert *et al.*, 2010). Our data so far confirm that we can modify the recruitment of immune cells to tissue following ethanol exposure, and that we can collect viable immune cells from PCLS. Although the model we have used does not deliver immune cells to the liver via the vasculature and does not incorporate physiological shear stress, adhesion events predominantly localize to endothelial sites in the parenchyma. The sinusoidal vascular bed is a major route for immune cell entry into the liver parenchyma (Shetty *et al.*, 2011; Xu *et al.*, 2008) from where recruited cells can subsequently migrate to sites in periportal areas. Data from our group confirm that molecular mechanisms of binding to sinusoidal endothelium dissected using this type of adhesion assay correlate well with our flow-based studies that model the effects of blood flow on binding to sinusoidal endothelium (Grant *et al.*, 2001; Liaskou *et al.*, 2011); thus, this system represents a good model for examining early immune cell recruitment following ethanol challenge. We shall extend these studies to determine the regulation of recruitment of specific lymphocytes such as natural killer T cells (Byun and Jeong, 2010) to the alcohol-exposed liver and also the effects of alcohol on the resident immune populations and further to evaluate the important potential of the human PCLS system as a screening tool for novel therapeutic compounds.

SUPPLEMENTARY DATA

Supplementary data are available online at http://toxsci.oxfordjournals.org/.

FUNDING

National Institutes of Health (5RO1AA014257) project to DHA and PFL to study human immune responses following alcohol exposure; Biotechnology and Biosciences Research Council case studentship with Unilever (BB/G529824/1 to P.L. for S.K.).

ACKNOWLEDGMENTS

We are grateful to our clinical colleagues and the generous patients at Queen Elizabeth Hospital in Birmingham for providing access to tissue samples.

REFERENCES

Aldridge, V., Garg, A., Davies, N., Bartlett, D. C., Youster, J., Beard, H., Kavanagh, D. P., Kalia, N., Frampton, J., Lalor, P. F., *et al.* (2012). Human mesenchymal stem cells are recruited to injured liver in a β1-integrin and CD44 dependent manner. *Hepatology* **56,** 1063–1073.

Andrade, M. C., Albernaz, M. J., Araújo, M. S., Santos, B. P., Teixeira-Carvalho, A., Faria, A. M., and Martins-Filho, O. A. (2009). Short-term administration of ethanol in mice deviates antigen presentation activity towards B cells. *Scand. J. Immunol.* **70,** 226–237.

Beamand, J. A., Price, R. J., Cunninghame, M. E., and Lake, B. G. (1993). Culture of precision-cut liver slices: Effect of some peroxisome proliferators. *Food Chem. Toxicol.* **31,** 137–147.

Bhogal, R. H., Hodson, J., Bartlett, D. C., Weston, C. J., Curbishley, S. M., Haughton, E., Williams, K. T., Reynolds, G. M., Newsome, P. N., Adams, D. H., *et al.* (2011). Isolation of primary human hepatocytes from normal and diseased liver tissue: A one hundred liver experience. *PLoS ONE* **6,** e18222.

Boyadjieva, N., and Sarkar, D. K. (1999). Effects of ethanol on basal and adenosine-induced increases in beta-endorphin release and intracellular cAMP levels in hypothalamic cells. *Brain Res.* **824,** 112–118.

Burra, P., Hubscher, S. G., Shaw, J., Elias, E., and Adams, D. H. (1992). Is the intercellular adhesion molecule-1/leukocyte function associated antigen 1 pathway of leukocyte adhesion involved in the tissue damage of alcoholic hepatitis? *Gut* **33,** 268–271.

Byun, J. S., and Jeong, W. I. (2010). Involvement of hepatic innate immunity in alcoholic liver disease. *Immune Netw.* **10,** 181–187.

Cazanave, S. C., and Gores, G. J. (2010). Mechanisms and clinical implications of hepatocyte lipoapoptosis. *Clin. Lipidol.* **5,** 71–85.

Chiva-Blanch, G., Urpi-Sarda, M., Llorach, R., Rotches-Ribalta, M., Guillén, M., Casas, R., Arranz, S., Valderas-Martinez, P., Portoles, O., Corella, D., *et al.* (2012). Differential effects of polyphenols and alcohol of red wine on the expression of adhesion molecules and inflammatory cytokines related to atherosclerosis: A randomized clinical trial. *Am. J. Clin. Nutr.* **95,** 326–334.

Clouzeau-Girard, H., Guyot, C., Combe, C., Moronvalle-Halley, V., Housset, C., Lamireau, T., Rosenbaum, J., and Desmoulière, A. (2006). Effects of bile acids on biliary epithelial cell proliferation and portal fibroblast activation using rat liver slices. *Lab. Invest.* **86,** 275–285.

Cohen, J. I., and Nagy, L. E. (2011). Pathogenesis of alcoholic liver disease: Interactions between parenchymal and non-parenchymal cells. *J. Dig. Dis.* **12,** 3–9.

Cohen, P. A., Mak, K. M., Rosman, A. S., Kessova, I., Mishin, V. M., Koivisto, T., and Lieber, C. S. (1997). Immunohistochemical determination of hepatic cytochrome P-4502E1 in formalin-fixed, paraffin-embedded sections. *Alcohol. Clin. Exp. Res.* **21,** 1057–1062.

Connors, S., Rankin, D. R., Gandolfi, A. J., Krumdieck, C. L., Koep, L. J., and Brendel, K. (1990). Cocaine hepatotoxicity in cultured liver slices: A species comparison. *Toxicology* **61,** 171–183.

Curbishley, S. M., Eksteen, B., Gladue, R. P., Lalor, P., and Adams, D. H. (2005). CXCR 3 activation promotes lymphocyte transendothelial migration across human hepatic endothelium under fluid flow. *Am. J. Pathol.* **167,** 887–899.

Donohue, T. M., Osna, N. A., and Clemens, D. L. (2006). Recombinant Hep G2 cells that express alcohol dehydrogenase and cytochrome P450 2E1 as a model of ethanol-elicited cytotoxicity. *Int. J. Biochem. Cell Biol.* **38,** 92–101.

Edwards, S., Lalor, P. F., Tuncer, C., and Adams, D. H. (2006). Vitronectin in human hepatic tumours contributes to the recruitment of lymphocytes in an alpha v beta3-independent manner. *Br. J. Cancer* **95,** 1545–1554.

Faubion, W. A., Guicciardi, M. E., Miyoshi, H., Bronk, S. F., Roberts, P. J., Svingen, P. A., Kaufmann, S. H., and Gores, G. J. (1999). Toxic bile salts induce rodent hepatocyte apoptosis via direct activation of Fas. *J. Clin. Invest.* **103,** 137–145.

Fernandez-Mateos, P., Jiménez-Ortega, V., Cano Barquilla, P., Cardinali, D. P., and Esquifino, A. I. (2012). Discontinuous versus continuous drinking of ethanol in peripubertal rats: Effect on 24-hour pattern of hypophyseal-gonadal axis activity and anterior pituitary oxidative stress. *Neuroendocrinology* **96,** 194–203.

Goddard, S., Youster, J., Morgan, E., and Adams, D. H. (2004). Interleukin-10 secretion differentiates dendritic cells from human liver and skin. *Am. J. Pathol.* **164,** 511–519.

Grant, A. J., Lalor, P. F., Hübscher, S. G., Briskin, M., and Adams, D. H. (2001). MAdCAM-1 expressed in chronic inflammatory liver disease supports mucosal lymphocyte adhesion to hepatic endothelium (MAdCAM-1 in chronic inflammatory liver disease). *Hepatology* **33,** 1065–1072.

Guyot, C., Combe, C., Balabaud, C., Bioulac-Sage, P., and Desmoulière, A. (2007a). Fibrogenic cell fate during fibrotic tissue remodelling observed in rat and human cultured liver slices. *J. Hepatol.* **46,** 142–150.

Guyot, C., Combe, C., Clouzeau-Girard, H., Moronvalle-Halley, V., and Desmoulière, A. (2007b). Specific activation of the different fibrogenic cells in rat cultured liver slices mimicking in vivo situations. *Virchows Arch.* **450,** 503–512.

Guyot, C., Lepreux, S., Combe, C., Sarrazy, V., Billet, F., Balabaud, C., Bioulac-Sage, P., and Desmoulière, A. (2010). Fibrogenic cell phenotype modifications during remodelling of normal and pathological human liver in cultured slices. *Liver Int.* **30,** 1529–1540.

Haseba, T., and Ohno, Y. (2010). A new view of alcohol metabolism and alcoholism–role of the high-Km Class III alcohol dehydrogenase (ADH3). *Int. J. Environ. Res. Public Health* **7,** 1076–1092.

Haydon, G., Lalor, P. F., Hubscher, S. G., and Adams, D. H. (2002). Lymphocyte recruitment to the liver in alcoholic liver disease. *Alcohol* **27,** 29–36.

Heinonen, J. T., Fisher, R., Brendel, K., and Eaton, D. L. (1996). Determination of aflatoxin B1 biotransformation and binding to hepatic macromolecules in human precision liver slices. *Toxicol. Appl. Pharmacol.* **136,** 1–7.

Iimuro, Y., Ikejima, K., Rose, M. L., Bradford, B. U., and Thurman, R. G. (1996). Nimodipine, a dihydropyridine-type calcium channel blocker, prevents alcoholic hepatitis caused by chronic intragastric ethanol exposure in the rat. *Hepatology* **24,** 391–397.

Jaruga, B., Hong, F., Kim, W. H., Sun, R., Fan, S., and Gao, B. (2004). Chronic alcohol consumption accelerates liver injury in T cell-mediated hepatitis: Alcohol dysregulation of NF-kappaB and STAT3 signaling pathways. *Am. J. Physiol. Gastrointest. Liver Physiol.* **287,** G471–G479.

Johnson, L. A., Clasper, S., Holt, A. P., Lalor, P. F., Baban, D., and Jackson, D. G. (2006). An inflammation-induced mechanism for leukocyte transmigration across lymphatic vessel endothelium. *J. Exp. Med.* **203,** 2763–2777.

Kirby, T. O., Rivera, A., Rein, D., Wang, M., Ulasov, I., Breidenbach, M., Kataram, M., Contreras, J. L., Krumdieck, C., Yamamoto, M., *et al.* (2004). A novel ex vivo model system for evaluation of conditionally

replicative adenoviruses therapeutic efficacy and toxicity. *Clin. Cancer Res.* **10,** 8697–8703.

Klassen, L. W., Thiele, G. M., Duryee, M. J., Schaffert, C. S., DeVeney, A. L., Hunter, C. D., Olinga, P., and Tuma, D. J. (2008). An in vitro method of alcoholic liver injury using precision-cut liver slices from rats. *Biochem. Pharmacol.* **76,** 426–436.

Knolle, P. A., Germann, T., Treichel, U., Uhrig, A., Schmitt, E., Hegenbarth, S., Lohse, A. W., and Gerken, G. (1999). Endotoxin down-regulates T cell activation by antigen-presenting liver sinusoidal endothelial cells. *J. Immunol.* **162,** 1401–1407.

Kono, H., Uesugi, T., Froh, M., Rusyn, I., Bradford, B. U., and Thurman, R. G. (2001). ICAM-1 is involved in the mechanism of alcohol-induced liver injury: Studies with knockout mice. *Am. J. Physiol. Gastrointest. Liver Physiol.* **280,** G1289–G1295.

Lalor, P. F., Curbishley, S. M., and Adams, D. H. (2010). Identifying homing interactions in T-cell traffic in human disease. *Methods Mol. Biol.* **616,** 231–252.

Lalor, P. F., Faint, J., Aarbodem, Y., Hubscher, S. G., and Adams, D. H. (2007). The role of cytokines and chemokines in the development of steatohepatitis. *Semin. Liver Dis.* **27,** 173–193.

Liaskou, E., Karikoski, M., Reynolds, G. M., Lalor, P. F., Weston, C. J., Pullen, N., Salmi, M., Jalkanen, S., and Adams, D. H. (2011). Regulation of mucosal addressin cell adhesion molecule 1 expression in human and mice by vascular adhesion protein 1 amine oxidase activity. *Hepatology* **53,** 661–672.

Liu, X., Zha, J., Nishitani, J., Chen, H., and Zack, J. A. (2003). HIV-1 infection in peripheral blood lymphocytes (PBLs) exposed to alcohol. *Virology* **307,** 37–44.

Martin, H., Sarsat, J. P., de Waziers, I., Housset, C., Balladur, P., Beaune, P., Albaladejo, V., and Lerche-Langrand, C. (2003). Induction of cytochrome P450 2B6 and 3A4 expression by phenobarbital and cyclophosphamide in cultured human liver slices. *Pharm. Res.* **20,** 557–568.

Massey, V. L., and Arteel, G. E. (2012). Acute alcohol-induced liver injury. *Front. Physiol.* **3,** 193.

Mortensen, B., and Dale, O. (1995). Effects of hypothermia on the elimination of ethanol, diazepam and oxazepam in rat liver slice incubations. *Acta Anaesthesiol. Scand.* **39,** 199–204.

Muller, D., Steinmetzer, P., Pissowotzki, K., and Glöckner, R. (2000). Induction of cytochrome P450 2B1-mRNA and pentoxyresorufin O-dependentylation after exposure of precision-cut rat liver slices to phenobarbital. *Toxicology* **144,** 93–97.

Naik, R. S., Mujumdar, A. M., and Ghaskadbi, S. (2004). Protection of liver cells from ethanol cytotoxicity by curcumin in liver slice culture in vitro. *J. Ethnopharmacol.* **95,** 31–37.

Neyrinck, A., Eeckhoudt, S. L., Meunier, C. J., Pampfer, S., Taper, H. S., Verbeeck, R. K., and Delzenne, N. (1999). Modulation of paracetamol metabolism by Kupffer cells: A study on rat liver slices. *Life Sci.* **65,** 2851–2859.

Oo, Y. H., Weston, C. J., Lalor, P. F., Curbishley, S. M., Withers, D. R., Reynolds, G. M., Shetty, S., Harki, J., Shaw, J. C., Eksteen, B., *et al.* (2010). Distinct roles for CCR4 and CXCR3 in the recruitment and positioning of regulatory T cells in the inflamed human liver. *J. Immunol.* **184,** 2886–2898.

Ozaki, M., Ogata, M., Nandate, K., Kawasaki, T., and Sata, T. (2007). The effects of ethanol on beta2-integrin and l-selectin on the surface of leukocytes in human whole blood. *J. Trauma* **63,** 770–774.

Price, R. J., Mistry, H., Wield, P. T., Renwick, A. B., Beamand, J. A., and Lake, B. G. (1996). Comparison of the toxicity of allyl alcohol, coumarin and menadione in precision-cut rat, guinea-pig, cynomolgus monkey and human liver slices. *Arch. Toxicol.* **71,** 107–111.

Ronis, M. J., Korourian, S., Yoon, S., Ingelman-Sundberg, M., Albano, E., Lindros, K. O., and Badger, T. M. (2004). Lack of sexual dimorphism in alcohol-induced liver damage (ALD) in rats treated chronically with ethanol-containing low carbohydrate diets: The role of ethanol metabolism and endotoxin. *Life Sci.* **75,** 469–483.

Sacanella, E., Estruch, R., Badía, E., Fernandez-Sola, J., Nicolás, J. M., and Urbano-Márquez, A. (1999). Chronic alcohol consumption increases serum levels of circulating endothelial cell/leucocyte adhesion molecules E-selectin and ICAM-1. *Alcohol Alcohol.* **34,** 678–684.

Saito, H., and Ishii, H. (2004). Recent understanding of immunological aspects in alcoholic hepatitis. *Hepatol. Res.* **30,** 193–198.

Schaffert, C. S., Duryee, M. J., Bennett, R. G., DeVeney, A. L., Tuma, D. J., Olinga, P., Easterling, K. C., Thiele, G. M., and Klassen, L. W. (2010). Exposure of precision-cut rat liver slices to ethanol accelerates fibrogenesis. *Am. J. Physiol. Gastrointest. Liver Physiol.* **299,** G661–G668.

Shetty, S., Weston, C. J., Oo, Y. H., Westerlund, N., Stamataki, Z., Youster, J., Hubscher, S. G., Salmi, M., Jalkanen, S., Lalor, P. F., *et al.* (2011). Common lymphatic endothelial and vascular endothelial receptor-1 mediates the transmigration of regulatory T cells across human hepatic sinusoidal endothelium. *J. Immunol.* **186,** 4147–4155.

Song, Z., Deaciuc, I., Song, M., Lee, D. Y., Liu, Y., Ji, X., and McClain, C. (2006). Silymarin protects against acute ethanol-induced hepatotoxicity in mice. *Alcohol. Clin. Exp. Res.* **30,** 407–413.

Tacke, F., Zimmermann, H. W., Berres, M. L., Trautwein, C., and Wasmuth, H. E. (2011). Serum chemokine receptor CXCR3 ligands are associated with progression, organ dysfunction and complications of chronic liver diseases. *Liver Int.* **31,** 840–849.

Thohan, S., Zurich, M. C., Chung, H., Weiner, M., Kane, A. S., and Rosen, G. M. (2001). Tissue slices revisited: Evaluation and development of a short-term incubation for integrated drug metabolism. *Drug Metab. Dispos.* **29,** 1337–1342.

van Geer, M. A., Kuhlmann, K. F., Bakker, C. T., ten Kate, F. J., Oude Elferink, R. P., and Bosma, P. J. (2009). Ex-vivo evaluation of gene therapy vectors in human pancreatic (cancer) tissue slices. *World J. Gastroenterol.* **15,** 1359–1366.

van Midwoud, P. M., Groothuis, G. M., Merema, M. T., and Verpoorte, E. (2010). Microfluidic biochip for the perifusion of precision-cut rat liver slices for metabolism and toxicology studies. *Biotechnol. Bioeng.* **105,** 184–194.

Wang, X., Douglas, S. D., Metzger, D. S., Guo, C. J., Li, Y., O'Brien, C. P., Song, L., Davis-Vogal, A., and Ho, W. Z. (2002). Alcohol potentiates HIV-1 infection of human blood mononuclear phagocytes. *Alcohol. Clin. Exp. Res.* **26,** 1880–1886.

Westerink, W. M., and Schoonen, W. G. (2007). Cytochrome P450 enzyme levels in HepG2 cells and cryopreserved primary human hepatocytes and their induction in HepG2 cells. *Toxicol. In Vitro* **21,** 1581–1591.

Wishnies, S. M., Parrish, A. R., Sipes, I. G., Gandolfi, A. J., Putnam, C. W., Krumdieck, C. L., and Brendel, K. (1991). Biotransformation activity in vitrified human liver slices. *Cryobiology* **28,** 216–226.

Wu, D., and Cederbaum, A. I. (2005). Oxidative stress mediated toxicity exerted by ethanol-inducible CYP2E1. *Toxicol. Appl. Pharmacol.* **207**(2 Suppl), 70–76.

Xu, X. D., Ueta, H., Zhou, S., Shi, C., Koga, D., Ushiki, T., and Matsuno, K. (2008). Trafficking of recirculating lymphocytes in the rat liver: Rapid transmigration into the portal area and then to the hepatic lymph. *Liver Int.* **28,** 319–330.

Xu, Y., Leo, M. A., and Lieber, C. S. (2003). Lycopene attenuates alcoholic apoptosis in HepG2 cells expressing CYP2E1. *Biochem. Biophys. Res. Commun.* **308,** 614–618.

Yeligar, S. M., Machida, K., Tsukamoto, H., and Kalra, V. K. (2009). Ethanol augments RANTES/CCL5 expression in rat liver sinusoidal endothelial cells and human endothelial cells via activation of NF-kappa B, HIF-1 alpha, and AP-1. *J. Immunol.* **183,** 5964–5976.

Zhang, T., Guo, C. J., Li, Y., Douglas, S. D., Qi, X. X., Song, L., and Ho, W. Z. (2003). Interleukin-1beta induces macrophage inflammatory protein-1beta expression in human hepatocytes. *Cell. Immunol.* **226,** 45–53.